Journal of Physics: Conference Series **501** (2014) 012003 doi:10.1088/1742-6596/501/1/012003

On the thermal instability in a horizontal rectangular porous channel heated from below by a constant flux

Antonio Barletta[1], Eugenia Rossi di Schio[1] and Leiv Storesletten[2]

[1]Department of Industrial Engineering, Alma Mater Studiorum Università di Bologna, Viale Risorgimento 2, 40136 Bologna, Italy

[2]Department of Mathematics, University of Agder, Postboks 422, 4604 Kristiansand, Norway

E-mail: antonio.barletta@unibo.it

Abstract. The onset of thermoconvective instability in a rectangular horizontal channel filled with a fluid-saturated porous medium is studied. The channel is heated from below with a constant flux. The top wall is maintained at a uniform constant temperature, while the lateral boundaries are permeable and perfectly conducting. The stability of the basic motionless state is analysed with respect to small-amplitude disturbances. The eigenvalue problem for the neutral stability condition is solved analytically for the normal modes. A closed-form expression is obtained for the implicit neutral stability relation between the Darcy-Rayleigh number and the longitudinal wave number. The critical condition, *viz.* the absolute minimum of the Darcy-Rayleigh number for the instability, is determined for different aspect ratios of the rectangular cross-section. The preferred modes under critical conditions are detected. It is found that the selected patterns of instability at the critical Rayleigh number may be two-dimensional, for slender or square cross-sections of the channel. On the other hand, instability is three dimensional when the critical width-to-height ratio, 1.350517, is exceeded.

1. Introduction

In the last decades, many authors investigated the onset of convection in a fluid saturated porous medium heated from below, starting from the pioneering papers by Horton and Rogers [1], and by Lapwood [2]. Nowadays, this topic is termed, in a wide sense, either Horton-Rogers-Lapwood problem, or Darcy-Bénard problem. Surveys on the main results obtained in this field were written by Rees [3], Tyvand [4], Nield and Bejan [5], Straughan [6], Barletta [7]. The Darcy-Bénard problem was originally formulated for an infinitely wide horizontal saturated porous layer in a motionless state, bounded by two horizontal, isothermal and impermeable walls maintained at different temperatures. In later investigations, various types of thermal boundary conditions, involving all possible combinations of isothermal and isoflux conditions, were analysed. Furthermore, the condition of a finite lateral width of the channel was analysed as well. The case of a horizontal porous channel with rectangular cross-section was studied by Sutton [8], Beck [9], and further explored by Nilsen and Storesletten [10].

Recently, Barletta and Storesletten [11] studied the onset of convection in a horizontal rectangular channel, bounded above and below with impermeable isothermal walls at different temperatures, but with partially conducting sidewalls. These authors carried out a three-dimensional linear stability analysis both for a channel with a longitudinal infinite length and for a finite longitudinal length. The linear disturbance equations were solved by Galerkin's method of

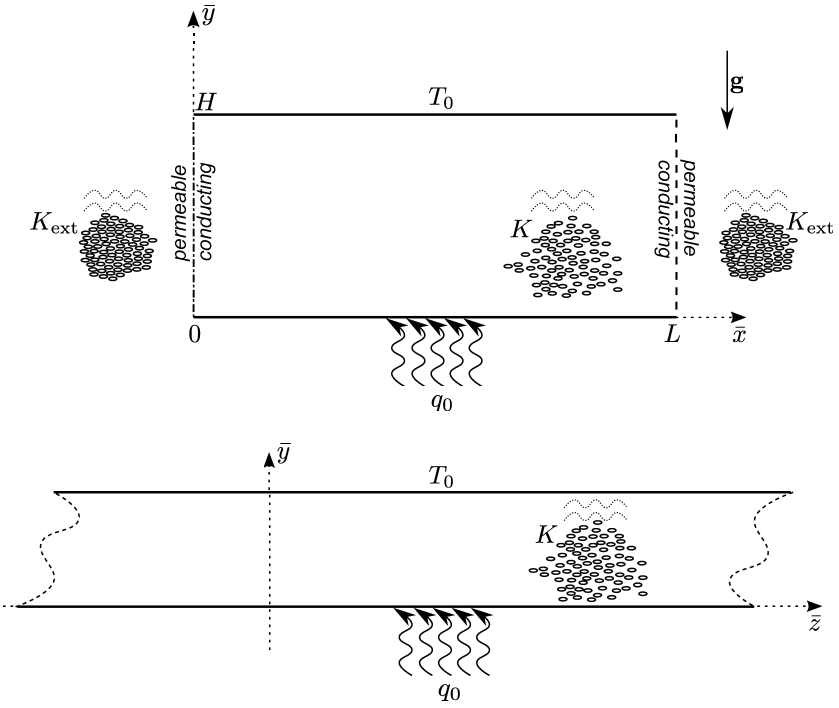

Figure 1. Sketch of the rectangular porous channel.

weighted residuals, as well as by a sixth-order Runge-Kutta method combined with the shooting method. The thermal behaviour of the vertical sidewalls was modelled through a Biot number associated with the convection to an external, thermally stratified, fluid environment.

The aim of the present paper is to extend the analysis presented in Ref. [11]. We will consider a horizontal rectangular porous channel, having infinite length in the longitudinal direction. The lower horizontal wall is impermeable and subject to an upward uniform heat flux, while the upper horizontal wall is impermeable and isothermal. The permeable side boundaries are assumed to be in perfect thermal and mechanical contact with an external porous reservoir, saturated by the same fluid and thermally stratified in the vertical direction, so that Dirichlet temperature and pressure conditions can be prescribed. The local momentum balance is modelled by Darcy's law, while the local energy balance is formulated by assuming local thermal equilibrium between the solid and the fluid phase. With the fluid that saturates the porous channel initially at rest, a three-dimensional linear stability analysis will be carried out. The governing equations for the linear disturbances of the basic state will be solved analytically. The neutral stability curves, as well as the critical values of the Darcy-Rayleigh number, will be determined for assigned values of the transverse aspect ratio.

2. Mathematical model

Let us devise a horizontal channel filled with a fluid saturated porous medium. In the following, the dimensional fields, coordinates, time and nabla operator are denoted by an overline. The channel is rectangular with height H and width L, and we choose a Cartesian coordinate system with the $\bar{y}-$ axis in the vertical direction and the $\bar{x}-$axis in the horizontal direction perpendicular to the channel $\bar{z}-$axis. The horizontal channel boundaries are at $\bar{y} = 0$ and $\bar{y} = H$, and the vertical boundaries at $\bar{x} = 0$ and $\bar{x} = L$ (see figure 1).

The components of the seepage velocity $\bar{\mathbf{u}}$, relative to the Cartesian set of coordinates $(\bar{x}, \bar{y}, \bar{z})$,

are denoted as $(\bar{u}, \bar{v}, \bar{w})$, respectively. Let us assume that the porous medium is homogeneous and isotropic, that the effect of viscous dissipation is negligible, and that the solid and fluid phases are in local thermal equilibrium. We assume the validity of Darcy's law and of the Oberbeck-Boussinesq approximation. Then, the local balance equations of mass, momentum and energy are written as

$$\begin{aligned} &\bar{\boldsymbol{\nabla}} \cdot \bar{\mathbf{u}} = 0, \\ &\frac{\mu}{K}\,\bar{\mathbf{u}} = -\bar{\boldsymbol{\nabla}}\bar{p} + \varrho\, g\, \beta\, \left(\bar{T} - T_0\right) \mathbf{e}_y, \\ &\sigma\,\frac{\partial \bar{T}}{\partial \bar{t}} + \bar{\mathbf{u}} \cdot \bar{\boldsymbol{\nabla}}\bar{T} = \alpha\, \bar{\nabla}^2 \bar{T}, \end{aligned} \tag{1}$$

where $\mathbf{g} = -g\,\mathbf{e}_y$ is the gravitational acceleration with $\mathbf{e}_y$ the unit vector along the vertical $\bar{y}-$axis, μ is the dynamic viscosity, K is the permeability, $\bar{p}$ is the dynamic pressure, *viz.* the local difference between the pressure and the hydrostatic pressure. Moreover, ρ is the reference density, β is the thermal expansion coefficient, $\bar{t}$ is time, $\bar{T}$ is temperature and T_0 is the reference temperature, α is the average thermal diffusivity, σ is the ratio between the average volumetric heat capacity of the fluid saturated porous medium and the volumetric heat capacity of the fluid.

The channel horizontal walls are impermeable, with the lower wall ($\bar{y} = 0$) subject to a positive uniform heat flux $q_0 = k\,\Delta T/H$, with k denoting the average thermal conductivity of the saturated porous medium. On the other hand, the upper wall ($\bar{y} = H$) is isothermal with temperature T_0. The lateral boundaries ($\bar{x} = 0, L$) are assumed to be perfectly permeable and in perfect thermal contact with an external porous reservoir saturated by the same fluid. The external reservoir is in a steady state thermally stratified in the vertical direction. The temperature field and the dynamic pressure field in the external reservoir are given by

$$\bar{T}_{\text{ext}}(\bar{y}) = T_0 + \Delta T\left(1 - \frac{\bar{y}}{H}\right), \tag{2a}$$

$$\bar{p}_{\text{ext}}(\bar{y}) = p_0 + \rho g \beta \Delta T\, \bar{y}\left(1 - \frac{\bar{y}}{2H}\right), \tag{2b}$$

where p_0 is a reference pressure. The permeability K_{ext} of the porous reservoir external to the rectangular channel is assumed to be much smaller than K, so that the steady state in the reservoir remains stable in spite of the possible onset of convection instability inside the porous channel.

On account of equations (2), the boundary conditions can be expressed as follows:

$$\begin{aligned} &\bar{v} = 0, \quad -k\,\frac{\partial \bar{T}}{\partial \bar{y}} = q_0, \qquad \text{on} \quad \bar{y} = 0, \quad 0 < \bar{x} < L, \\ &\bar{v} = 0, \quad \bar{T} = T_0, \qquad \text{on} \quad \bar{y} = H, \quad 0 < \bar{x} < L, \\ &\bar{p} = \bar{p}_{\text{ext}}(\bar{y}), \quad \bar{T} = \bar{T}_{\text{ext}}(\bar{y}), \qquad \text{on} \quad \bar{x} = 0, L, \quad 0 < \bar{y} < H. \end{aligned} \tag{3}$$

The dimensionless quantities are defined such that

$$\begin{aligned} &(\bar{x}, \bar{y}, \bar{z}) = (x,\, y,\, z)\, H, \quad \bar{\mathbf{u}} = (\bar{u}, \bar{v}, \bar{w}) = (u,\, v,\, w)\,\frac{\alpha}{H} = \mathbf{u}\,\frac{\alpha}{H}, \\ &\bar{\boldsymbol{\nabla}} = \frac{1}{H}\boldsymbol{\nabla}, \quad \bar{T} = T_0 + \frac{q_0\, H}{k}\,T, \quad \bar{p} = p_0 + \frac{\mu\,\alpha}{K}\,p, \\ &\bar{t} = \frac{\sigma\, H^2}{\alpha}\,t, \quad s = \frac{L}{H}. \end{aligned} \tag{4}$$

The governing equations (1) can thus be rewritten in a dimensionless form as

$$\boldsymbol{\nabla} \cdot \mathbf{u} = 0, \tag{5a}$$
$$\mathbf{u} = -\boldsymbol{\nabla} p + R\, T\, \mathbf{e}_y, \tag{5b}$$
$$\frac{\partial T}{\partial t} + \mathbf{u} \cdot \boldsymbol{\nabla} T = \nabla^2 T, \tag{5c}$$

where R is the Darcy-Rayleigh number, given by

$$R = \frac{\varrho g \beta q_0 K H^2}{k \mu \alpha}. \tag{6}$$

The boundary conditions (2) and (3) can be rewritten as

$$\begin{aligned} &v = 0, \quad \frac{\partial T}{\partial y} = -1, \qquad \text{on} \quad y = 0, \quad 0 < x < s, \\ &v = 0, \quad T = 0, \qquad \text{on} \quad y = 1, \quad 0 < x < s, \\ &p = R\, y \left(1 - \frac{y}{2}\right), \quad T = 1 - y, \qquad \text{on} \quad x = 0, s, \quad 0 < y < 1. \end{aligned} \tag{7}$$

3. Basic solution and linear disturbances

A stationary solution of equations (5) and (7) is given by

$$u_b = v_b = w_b = 0, \quad T_b = 1 - y, \quad p_b = R\, y \left(1 - \frac{y}{2}\right). \tag{8}$$

where b stands for *basic solution*. We can adopt a pressure-temperature formulation of equations (5) by substituting equation (5b) into (5a) and (5c), thus yielding

$$\begin{aligned} &\nabla^2 p = R \frac{\partial T}{\partial y}, \\ &\nabla^2 T = \frac{\partial T}{\partial t} - \boldsymbol{\nabla} p \cdot \boldsymbol{\nabla} T + R\, T \frac{\partial T}{\partial y}. \end{aligned} \tag{9}$$

The boundary conditions now become

$$\begin{aligned} &\frac{\partial p}{\partial y} = R\, T, \quad \frac{\partial T}{\partial y} = -1, \qquad \text{on} \quad y = 0, \quad 0 < x < s, \\ &\frac{\partial p}{\partial y} = 0, \quad T = 0, \qquad \text{on} \quad y = 1, \quad 0 < x < s, \\ &p = R\, y \left(1 - \frac{y}{2}\right), \quad T = 1 - y, \qquad \text{on} \quad x = 0, s, \quad 0 < y < 1. \end{aligned} \tag{10}$$

We perturb the basic solution (8) with small amplitude disturbances, defined by

$$p = p_b + \varepsilon\, P, \qquad T = T_b + \varepsilon\, \theta. \tag{11}$$

Following the usual linear stability analysis, we substitute equation (11) into (9) and we neglect the terms of order ε^2. Thus, we obtain

$$\begin{aligned} &\nabla^2 P = R \frac{\partial \theta}{\partial y}, \\ &\nabla^2 \theta = \frac{\partial \theta}{\partial t} - R\, \theta + \frac{\partial P}{\partial y}, \end{aligned} \tag{12}$$

to be subjected to the boundary conditions

$$\begin{aligned} &\frac{\partial P}{\partial y} = R\,\theta, \quad \frac{\partial \theta}{\partial y} = 0, \qquad \text{on} \quad y = 0, \quad 0 < x < s, \\ &\frac{\partial P}{\partial y} = 0, \quad \theta = 0, \qquad \text{on} \quad y = 1, \quad 0 < x < s, \\ &P = 0, \quad \theta = 0, \qquad \text{on} \quad x = 0, s, \quad 0 < y < 1. \end{aligned} \tag{13}$$

4. Normal modes

Due to the principle of exchange of stabilities, the study of the neutral stability condition is relative to the time-independent solutions of equations (12). Following the usual normal mode decomposition, we may write

$$\begin{aligned} P(x,y,z) &= f_n(y)\,\sin\!\left(\frac{n\pi x}{s}\right)\cos(az), \\ \theta(x,y,z) &= h_n(y)\,\sin\!\left(\frac{n\pi x}{s}\right)\cos(az), \end{aligned} \tag{14}$$

where $n = 1, 2, \dots$, and a is the dimensionless wave number in the $z-$direction. We substitute equation (14) into (12) so that we obtain

$$f_n'' - \left(a^2 + \frac{n^2\pi^2}{s^2}\right) f_n - R\,h_n' = 0, \tag{15a}$$

$$h_n'' - \left(a^2 + \frac{n^2\pi^2}{s^2} - R\right) h_n - f_n' = 0, \tag{15b}$$

with the boundary conditions

$$\begin{aligned} &f_n' = R\,h_n, \quad h_n' = 0, \qquad \text{on} \quad y = 0, \\ &f_n' = 0, \quad h_n = 0, \qquad \text{on} \quad y = 1. \end{aligned} \tag{16}$$

In equations (15) and (16), primes denote derivatives with respect to y. Let us define

$$\varphi_n(y) = -f_n'(y) + R\,h_n(y), \tag{17a}$$

$$b_n^2 = a^2 + \frac{n^2\pi^2}{s^2}, \tag{17b}$$

then (15) and (16) can be reformulated as

$$\varphi_n'' - b_n^2\varphi_n + R\,b_n^2 h_n = 0, \tag{18a}$$

$$h_n'' - b_n^2 h_n + \varphi_n = 0, \tag{18b}$$

with the boundary conditions

$$\begin{aligned} &\varphi_n = 0, \quad h_n' = 0, \qquad \text{on} \quad y = 0, \\ &\varphi_n = 0, \quad h_n = 0, \qquad \text{on} \quad y = 1. \end{aligned} \tag{19}$$

5. Analytical solution

The solution of equations (18) and (19) can be determined by employing the usual method of the characteristic equation. Since the boundary value problem is homogeneous, the solution is to be determined up to an arbitrary scale factor. It is not restrictive to set the latter so that

$$h_n(0) = 1. \tag{20}$$

Then, we may write

$$\begin{aligned} \varphi_n(y) &= b_n\sqrt{R}\left[A_n\,\sin(\lambda_n y) + \frac{1}{2}\,\cos(\lambda_n y) + \frac{A_n\lambda_n}{\eta_n}\sinh(\eta_n y) - \frac{1}{2}\,\cosh(\eta_n y)\right], \\ h_n(y) &= A_n\,\sin(\lambda_n y) + \frac{1}{2}\,\cos(\lambda_n y) - \frac{A_n\lambda_n}{\eta_n}\sinh(\eta_n y) + \frac{1}{2}\,\cosh(\eta_n y)\,, \end{aligned} \tag{21}$$

where

$$\begin{aligned} \lambda_n &= \sqrt{b_n\left(\sqrt{R} - b_n\right)}, \\ \eta_n &= \sqrt{b_n\left(\sqrt{R} + b_n\right)}, \\ A_n &= \frac{\eta_n\left(\cosh\eta_n - \cos\lambda_n\right)}{2\left(\eta_n\sin\lambda_n + \lambda_n\sinh\eta_n\right)}. \end{aligned} \tag{22}$$

Equations (21) and (22) ensure that (18) and (20) are satisfied, together with the boundary conditions, given by Eq. (19): $\varphi_n(0) = \varphi_n(1) = 0$ and $h_n'(0) = 0$. On the other hand, the last boundary condition, $h_n(1) = 0$, leads to the dispersion relation

$$\frac{\lambda_n\sinh\eta_n\cos\lambda_n + \eta_n\cosh\eta_n\sin\lambda_n}{\eta_n\sin\lambda_n + \lambda_n\sinh\eta_n} = 0. \tag{23}$$

Equations (17b), (22) and (23) allow one to plot the neutral stability curves in the parametric plane (a, R), for any given aspect ratio s.

6. Discussion of the results

The dispersion relation (23) can be displayed in the parametric plane (b_n, R). Obviously, if we do not specify the modal number n and the transverse aspect ratio s, the parameter b_n is nothing but a redefined wave number that can vary continuously over the set of positive real numbers. In this case, for the sake of simplicity, we denote b_n with b and plot equation (23) in the plane (b, R). This plot is shown in figure 2. There are two disconnected curves, each one displaying a minimum. The lower curve has a minimum for

$$b = 2.326215, \qquad R = 27.09763, \tag{24}$$

while the upper curve has a minimum for

$$b = 5.468656, \qquad R = 132.3633. \tag{25}$$

We note that the lower curve is that describing the transition to instability. When R is below this curve, for a given b, we have in fact linear stability. Then, the pair (b, R) given by equation (24) is the critical pair for the onset of instability. We mention that the same critical value of R was found by Ribando and Torrance [12], and more recently by Wang [13] on studying

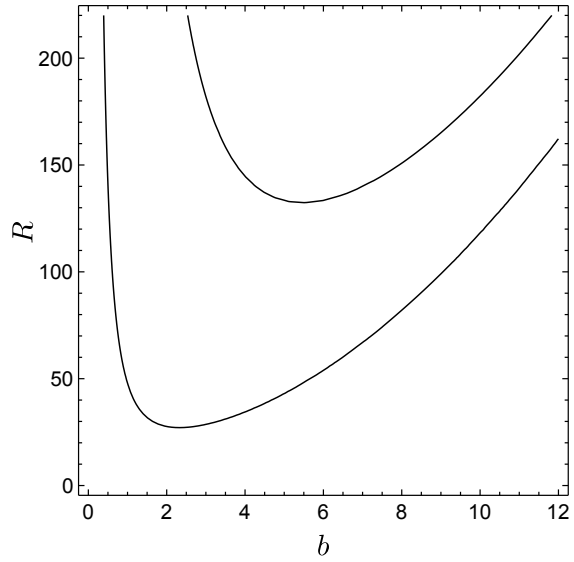

Figure 2. Neutral stability curves in the plane (b, R).

the stability of a saturated rectangular porous box with lateral impermeable and adiabatic boundaries, upper horizontal wall maintained at constant temperature, and lower horizontal wall heated by a constant flux.

Due to the lateral confinement, with a given aspect ratio s, the longitudinal wave number a is related to b_n through equation (17b), so that we can plot the neutral stability curves with respect to a for prescribed modal numbers n. These plots are displayed in figures 3-8, relative to the aspect ratios $s = 1/2,\ 3/4,\ 1,\ 3/2,\ 2,\ 5/2$. The aspect ratio $s = 1$ (figure 5) is for a square channel, while $s < 1$ (figures 3 and 4) is for a slender rectangular channel, and $s > 1$ (figures 6, 7 and 8) is for a shallow rectangular channel.

Figures 3-5 show that the most unstable modes are those with $n = 1$ and that the onset of convection takes place for vanishingly small wave numbers, meaning $z-$independent or two-dimensional modes. In particular, for $s = 1/2,\ 3/4,\ 1$ the critical wave number is $a_c = 0$ and the critical values of R are $R_c = 57.33,\ 35.83,\ 29.21$, respectively. This behaviour changes slightly in figure 6 where, even if the least stable modes are still for $n = 1$, we have a nonvanishing critical wave number $a_c = 1.012$ and a critical Darcy-Rayleigh number $R_c = 27.10$, *viz.* just the same value of R reported in (24). We mention that the value $a_c = 1.012$ arises just by taking the value of b from equation (25) and employing (17) with $n = 1$ and $s = 3/2$. The transition from a condition with $a_c = 0$ to one with $a_c > 0$ arises with a value of s intermediate between $s = 1$ (figure 5) and $s = 3/2$ (figure 6). A precise evaluation of this transition aspect ratio yields

$$s = 1.350517. \tag{26}$$

Below this aspect ratio, the onset of convection is two-dimensional ($z-$independent), while for higher aspect ratios the selected modes at neutral stability are three-dimensional. Relative to a shallow channel, figures 7 and 8 show that the modes with $n = 1$ are not the most unstable over the whole range of a, but only for sufficiently large wave numbers: $a > 0.6290$ and $a > 1.401$ for $s = 2$ and $s = 5/2$, respectively. For smaller wave numbers, the modes with $n = 2$ prevail. Anyway, the absolute minimum of R for neutral stability takes place for $n = 1$ in both cases, and this is for a nonvanishing critical wave number. Another interesting feature displayed by figures 5-8 is that, on increasing the aspect ratio s, the neutral stability curves with $n = 1, 2, 3$ become

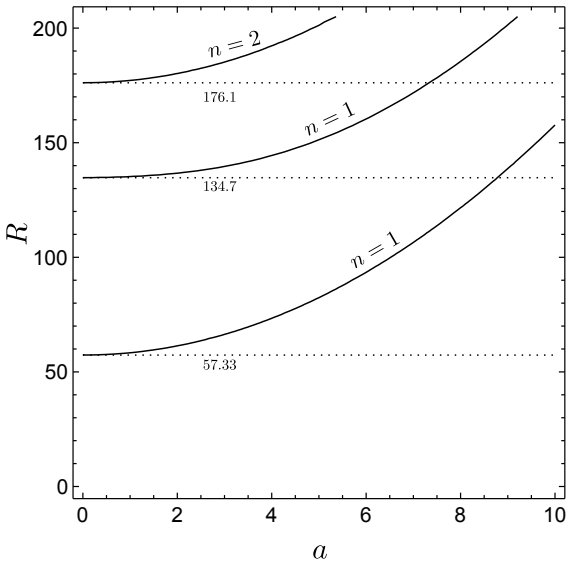

Figure 3. Neutral stability curves in the plane (a, R) for $s = 1/2$. The dotted lines denote the minimum of each branch.

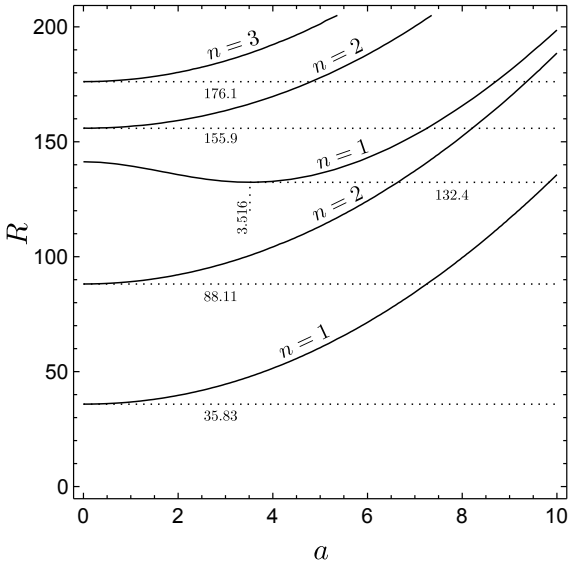

Figure 4. Neutral stability curves in the plane (a, R) for $s = 3/4$. The dotted lines denote the minimum of each branch.

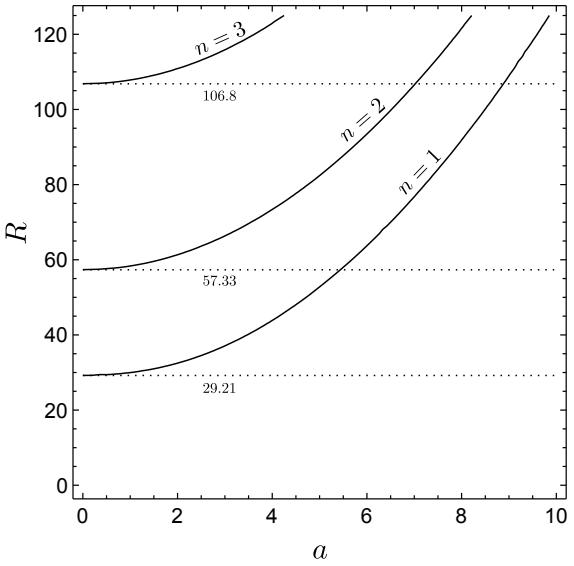

Figure 5. Neutral stability curves in the plane (a, R) for $s = 1$. The dotted lines denote the minimum of each branch.

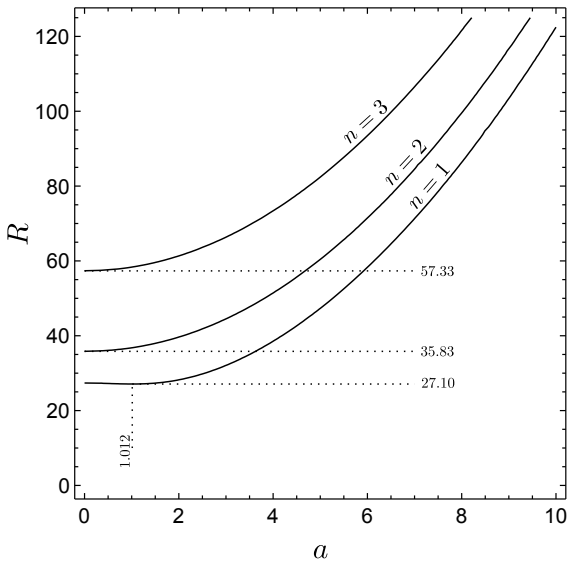

Figure 6. Neutral stability curves in the plane (a, R) for $s = 3/2$. The dotted lines denote the minimum of each branch.

closer and closer, meaning an easier transition between different modes at slightly supercritical conditions.

7. Conclusions

The stability versus small-amplitude disturbances of the steady motionless state in a horizontal rectangular channel containing a fluid-saturated porous material has been investigated. A special case is described where the heating from below is modelled by a uniform flux and the cooling

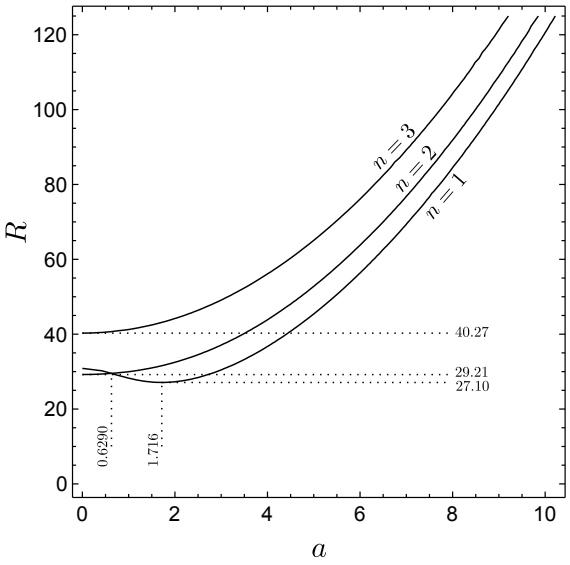

Figure 7. Neutral stability curves in the plane (a, R) for $s = 2$. The dotted lines denote the minimum of each branch and the intersection between different branches.

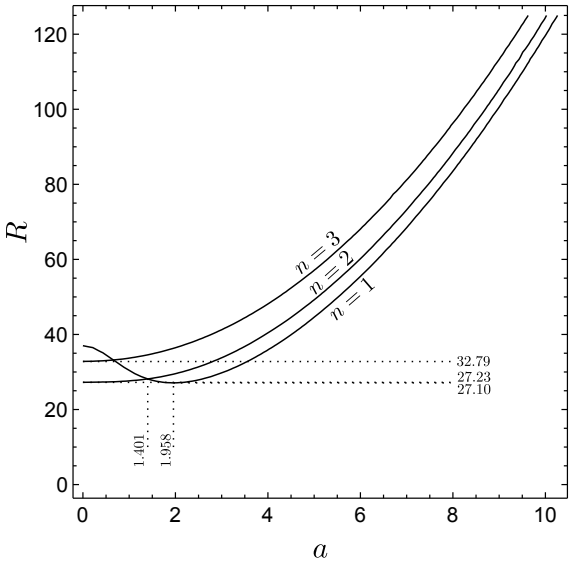

Figure 8. Neutral stability curves in the plane (a, R) for $s = 5/2$. The dotted lines denote the minimum of each branch and the intersection between different branches.

from above is modelled by a uniform temperature. The lateral confinement is by thermal and mechanical contact with a saturated porous reservoir in a steady state with vertical thermal stratification.

Darcy's law and the Oberbeck-Boussinesq approximation are adopted for modelling the buoyant flow. The dimensionless parameters governing the onset of the instability are the Darcy-Rayleigh number, R, and the width-to-height aspect ratio, s. An analytical solution of the disturbance equations has been found for the normal modes. These modes are labelled by the natural number, n, that yields the number of nodes in the sinusoidal temperature distribution along the transverse horizontal direction, namely along the $x-$axis.

A study of the neutral stability curves has been carried out for different aspect ratios ranging from $s = 1/2$ to $s = 5/2$. The main feature emerged from this study is that the modes with $n = 1$ are preferred at onset of convection. However, the critical condition, defined as the absolute minimum of R leading to instability, may be displayed either with two-dimensional instability patterns or three-dimensional patterns. The former are rolls invariant along the longitudinal $z-$direction. The three-dimensional patterns are preferred at the onset of instability when the aspect ratio is sufficiently large, *viz.* exceeding the threshold value $s = 1.350517$. Under these conditions, the absolute minimum of R leading to instability is the critical value $R = 27.09763$.

Opportunities for future developments of this study are foreseen. The effect of a finite longitudinal length along the $z-$axis is yet to be analysed. With this respect, specific assumptions about the planes, $z = constant$, bounding longitudinally the channel are to be made. Another possible future development is relative to the role played by the type of lateral confinement. We have shown that permeable and perfectly conducting side-boundaries lead to an analytical solution of the linear stability problem. The closely related case of impermeable and perfectly conducting sidewalls does not allow an analytical solution, and linear stability can be discussed only by means of a numerical solution of the governing equations for the disturbances. This challenging problem is a natural extension of the present analysis.

Acknowledgments
This work was financially supported by Italian government, MIUR grant PRIN-2009KSSKL3.

References
[1] Horton C W and Rogers F T 1945 *J Appl Phys* **16** 367–370
[2] Lapwood E R 1948 *Math Proc Cambridge* **44** 508–521
[3] Rees D A S 2000 *Handbook of Porous Media* ed Vafai K and Hadim H A (New York: CRC Press) chap 12, pp 521–558
[4] Tyvand P A 2002 *Transport Phenomena in Porous Media II* ed Ingham D B and Pop I (New York: Pergamon) chap 4, pp 82–112
[5] Nield D A and Bejan A 2006 *Convection in Porous Media* 3rd ed (New York: Springer)
[6] Straughan B 2008 *Stability and Wave Motion in Porous Media* (New York: Springer)
[7] Barletta A 2011 *Heat Transfer in Multi–Phase Materials* ed Öchsner A and Murch G E (New York: Springer) pp 381–414
[8] Sutton F M 1970 *Phys Fluids* **13** 1931–1934
[9] Beck J L 1972 *Phys Fluids* **15** 1377–1383
[10] Nilsen T and Storesletten L 1990 *J Heat trans-T ASME* **112** 396–401
[11] Barletta A and Storesletten L 2012 *Int J Therm Sci* **55** 1–15
[12] Ribando R J and Torrance K E 1976 *J Heat trans-T ASME* **98** 42–48
[13] Wang C Y 1999 *Phys Fluids* **11** 1673–1675